

# Higher-order vortex solitons, multipoles, and supervortices on a square optical lattice

Hidetsugu Sakaguchi<sup>1</sup> and Boris A. Malomed<sup>2</sup>

<sup>1</sup> Department of Applied Science for Electronics and Materials,  
Interdisciplinary Graduate School of Engineering Sciences,  
Kyushu University, Kasuga, Fukuoka 816-8580, Japan

<sup>2</sup> Department of Interdisciplinary Studies,  
School of Electrical Engineering, Faculty of Engineering,  
Tel Aviv University, Tel Aviv 69978, Israel

November 10, 2018

## Abstract

We predict new generic types of vorticity-carrying soliton complexes in a class of physical systems including an attractive Bose-Einstein condensate in a square optical lattice (OL) and photonic lattices in photorefractive media. The patterns include ring-shaped higher-order vortex solitons and supervortices. Stability diagrams for these patterns, based on direct simulations, are presented. The vortex ring solitons are stable if the phase difference  $\Delta\phi$  between adjacent solitons in the ring is larger than  $\pi/2$ , while the supervortices are stable in the opposite case,  $\Delta\phi < \pi/2$ . A qualitative explanation to the stability is given.

Recent experimental observations of two-dimensional (2D) solitons [1] and localized vortices [2] in photonic lattices in self-focusing photorefractive crystals (PRCs), and prediction of similar structures in the 2D Gross-Pitaevskii equation (GPE) for a self-attractive Bose-Einstein condensate (BEC) loaded into the square optical lattice (OL) [3, 4], have drawn interest to solitons of this type, including vorticity-carrying ones. Vortex solitons of the gap type have also been predicted in the repulsive GPE with the square OL [9, 10], including higher-order ones, with the vorticity  $S = 2$  [10]. However, the results which were reported thus far for the self-focusing media, both saturable and cubic, pertain solely to the vortices with  $S = 1$  (including strongly deformed ones [11]). In this work, we present stable vortex solitons with higher values of  $S$  and more complex vortex patterns, which suggests a possibility to create them in the experiment. We report the results for both BEC and PRC models, which attests to their generic character. It is relevant to mention that, in discrete models, which may be considered as a limiting case corresponding to a very strong OL, with

attraction and repulsion alike, both 2D and 3D vortex solitons with  $S = 2$  are unstable, but the ones with  $S = 3$  have their stability region [12].

In a moderately strong OL, we find stable vortex solitons with higher vorticities  $S$  and their counterparts in the form of quadrupole solitons (in the discrete model, the latter ones may be stable too [12]). The vortices with large  $S$  feature a ring shape, resembling vorticity-carrying “soliton necklaces”, that were recently studied in diverse spatially uniform [13] models, but, on the contrary to those models, the ring-shaped vortices on the square lattice are true stationary states, rather than slowly disintegrating quasi-patterns in the free space (recently, zero-vorticity necklaces and other soliton complexes were predicted and observed in Kerr and PRC media with a photonic lattice [14]). We also construct another generic type of stable structures that we call “supervortices” [15], i.e., ring-shaped (or densely packed) arrays of individual compact vortices with  $s = 1$ , arranged so that the ring itself carries global vorticity ( $s$  pertains to the intrinsic vorticity of an individual vortex in the array, to distinguish it from  $S$  referring to the global vorticity imprinted into the array). Although the ring-shaped supervortices may formally resemble dark-soliton vortex necklaces in external traps [16], they have never been considered before, as the individual solitary-wave vortex is unstable without the OL.

In the normalized form, the two-dimensional (2D) GPE with the negative atomic scattering length and square-OL potential is [3]

$$i\psi_t + (1/2)\nabla^2\psi + |\psi|^2\psi + \varepsilon [\cos(2x) + \cos(2y)]\psi = 0, \quad (1)$$

where  $\psi(x, y, t)$  is the BEC wave function, the OL period is scaled to be  $\pi$ , and  $\varepsilon$  is the OL strength, in units of the respective recoil energy. The vertical coordinate is excluded, assuming tight confinement in the third direction, which is readily provided by light sheets [5]. As is known (see, e.g., Ref. [6]), the underlying three-dimensional GPE with a negative scattering length of atomic collisions,  $a < 0$ , can be reduced to its 2D counterpart (1), provided that the transverse quantum pressure is much stronger than the self-attraction (which precludes the collapse). In other words, the energy of the atom with the mass  $m$  in the ground state of the vertical trap with a size  $a_z$ ,  $E_0^{(z)} \simeq \hbar^2 / (2ma_z^2)$ , must be much larger than the contribution of the attraction between atoms to the atomic chemical potential,  $\Delta\mu \simeq -2\pi\hbar^2 (a/m)n$ , where  $n$  is the three-dimensional density of atoms. Thus, the 2D GPE equation for the self-attractive condensate is relevant under the condition  $n \ll (4\pi a_z^2 a)^{-1}$ , which can be readily met in the experiment (in particular,  $a$  can be very small in  ${}^7\text{Li}$  [7]). In fact, this condition can be relaxed due to the stabilizing effect of the OL potential in Eq. (1).

Equation (1) does not include the external trapping (parabolic) potential, as we aim to look for patterns whose stability does not depend on the presence of the trap. An equation governing the spatial evolution of the amplitude  $\psi(x, y, z)$  of the probe beam in the PRC with a square photonic lattice of strength  $I_0$  differs

from Eq. (1) by the presence of saturation [1, 8],

$$i\psi_z + (1/2)\nabla^2\psi + \frac{\psi}{1 + I_0[\cos(Kx) + \cos(Ky)]^2 + |\psi|^2} \quad (2)$$

(strictly speaking, PRCs feature anisotropy, but in crystals used in work [1] the anisotropy is very weak and may be neglected). Stationary solutions with chemical potential  $\mu$  are looked for as  $\psi(x, y, t) = e^{-i\mu t}\Psi(x, y)$ , where the function  $\Psi$  is, generally, complex (in the PRC model,  $-\mu$  is the propagation constant). In this notation, the solutions depend on two parameters: the lattice strength,  $\varepsilon$  or  $I_0$ , and the norm (number of atoms/total power of the light signal),  $N = \int |\Psi(x, y)|^2 dx dy$ .

Equations (1) and (2) represent a class of models that extend to other physical media, such as nonlinear photonic crystals and photonic-crystal fibers [17]. The results reported below are valid for all these models, i.e., they suggest, in particular, the existence of stable vortex complexes of the new types in the photonic crystals as well (a vortex with  $s = 1$  was very recently predicted in photonic-crystal fibers [18]).

We built patterns with vorticity  $S$  as sets of  $M$  stable “single-cell” solitons with  $s = 0$ , or compact vortices with  $s = 1$ , by imprinting onto the set a phase distribution with the phase shift  $\Delta\phi = 2\pi S/M$  between adjacent solitons. The stability of the resulting states was tested in direct simulations. Initial shapes of the building blocks with  $s = 0$  and  $s = 1$  were taken as numerical solutions of the axially symmetric GPE with an *ad hoc* potential,  $U(r) = -\varepsilon \cos(2r)$  for  $0 < r < \pi/2$ , and  $U(r) \equiv \varepsilon$  for  $r > \pi/2$ , where  $r \equiv \sqrt{x^2 + y^2}$ , and  $\varepsilon$  is the same as in Eq. (1) And small random perturbations were further added. In cases of stabilities, it was observed that the shapes and structures of the vortex and supervortex composed of the building blocks changed hardly in time. It implies the vortex and supervortex structures are rather stable, since our initial conditions are slightly deviated from the exact stationary solutions. On the contrary, the vorticity-carrying phase pattern in unstable states is quickly replaced by an evidently chaotic distribution of phase, and shows no trend to relax into any simple configuration. The phase instability produces little effect on the amplitude shape of the pattern. That is, the profile of  $|\phi|$  has hardly changed in time.

Following this procedure, a stable vortex in Eq. (1) with  $S = 1, 2, 3$  and 4 were created using eight solitons surrounding an empty central cell. We have found that a vortex with  $S = 3$  is definitely stable, the one with  $S = 2$  is marginally stable. The “marginal stability” features the very slowly (linearly) growing perturbation in the phase configuration. Further, vortex solitons were also constructed based on 12 single-cell solitons surrounding a cluster of four empty cells. In the latter case, the vortices are stable for  $S = 4, 5$ , and 6. A stable vortex with  $S = 4$  is shown in Figs. 1(a) and (b). Monitoring the rotation of the local phase vector, which is defined as one with the components  $(\text{Re}\{\psi\}/|\psi|, \text{Im}\{\psi\}/|\psi|)$ , along a closed path in the counter-clockwise direction in Fig. 1(b), it is easy to see that the corresponding net change of the field’s phase is indeed  $\Delta\phi = 8\pi$ , corresponding to  $S = 4$ .

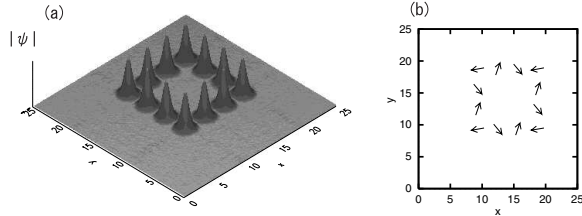


Figure 1: (a) A stable vortex soliton with  $S = 4$  and  $N = 33.4$ ; the field  $|\psi(x, y)|$  is plotted. (b) The field of the local phase vector,  $(\text{Re}\{\psi\}/|\psi|, \text{Im}\{\psi\}/|\psi|)$ , at centers of the constituent solitons for the vortex complex in (a). In all the cases shown here,  $\varepsilon = 3$ .

The existence and stability of these solitons depend on  $S$ , norm  $N$ , and  $\varepsilon$ . Keeping  $\varepsilon = 3$ , and varying both  $N$  and  $S$ , in the right part of Fig. 2 we summarize stability results for the vortex solitons of Eq. (1) based on the ring-shaped array of 12 single-cell solitons. For the judgement of the stability, we have calculated the time evolution of the maximum amplitude of  $|\psi|$  to check the collapse, and the time evolution of the root mean square of  $\Delta\phi - 2\pi S/12$  for the 12 single-cell solitons to investigate the phase instability, where  $\Delta\phi$  is the phase difference between adjacent solitons. The numerical simulation was performed until  $t = 150$ . We have constructed the stability diagram for the vortex solitons in Fig. 2 from these two kinds of time evolutions. For all  $S$ , the pattern collapses (each individual soliton suffers, as usual, catastrophic self-compression) if  $N$  exceeds a critical value,  $N_{\text{cr}} = 68.2$ , that virtually does not depend on  $S$ . This can be easily understood, taking into regard that, in the present notation, the critical norm for the onset of the collapse of an individual soliton in the 2D free-space nonlinear Schrödinger equation is  $N_{\text{cr}}^{(\text{NLS})} \approx 5.84$  [19], hence for the set of 12 pulses it predicts  $N_{\text{cr}} \approx 70.1$ . The small difference from the actual value,  $N_{\text{cr}} = 68.2$ , is due to the OL. For  $N < N_{\text{cr}}$ , all the patterns with  $S < 3$  are unstable, while the one with  $S = 3$  is marginal.

The above results for the vortices based on the ring-shaped arrays of 4, 8 and 12 single-cell solitons suggest that the stability is not determined by the vorticity  $S$  itself, but rather by the phase difference  $\Delta\phi$  between adjacent cells. All the vortex complexes built as described above are stable for  $\Delta\phi > \pi/2$  (including the quadrupoles, for which  $\Delta\phi = \pi$ ), being marginal for  $\Delta\phi = \pi/2$ . These inferences can be easily explained. Indeed, it is well known that sufficiently separated 2D solitons with the phase difference  $\Delta\phi$  interact repulsively if  $\Delta\phi > \pi/2$ , and attractively if  $\Delta\phi < \pi/2$ . On the other hand, it is also known that bound states of lattice solitons may be stable only in the case of repulsion [20]. Thus, the ring arrays trapped on the lattice have a chance to be stable just in the case of  $\Delta\phi > \pi/2$ .

It may be relevant to look at several fundamental vortices with  $S = 1$  studied

before from the same perspective. Baizakov et al. found the fundamental vortex with  $S = 1$ , which is arranged as a complex of four major and four minor peaks surrounding a central cell of the OL (see Fig.3(b) in [3]) and they showed that the vortex is stable by direct numerical analysis [3]. Alexander et al. found numerically a (stable) vortex with  $S = 1$  constructed of 4 single cell solitons for the PRC model [11], where the phase difference is  $\Delta\phi = \pi/2$ . Yang studied the linear stability of the vortex with  $S = 1$  and found that the vortex is stable in an intermediate range of peak amplitude and it is unstable outside of the parameter range [8]. We have found that the vortex with  $S = 1$  constructed of 4 single cell solitons is marginally stable (very weakly unstable) judging from the time evolution of the phase configuration. However, the amplitude profile  $|\psi|$  keeps the initial profile stably and the vortex structure is not broken until  $t = 150$  for the parameter value of  $\varepsilon = 3$ . In any way, the marginal case of  $\Delta\phi = \pi/2$  seems to be delicate and might need further investigation. However, we do not study it more in detail in this paper, because the main topics are higher-order vortex solitons and supervortices.

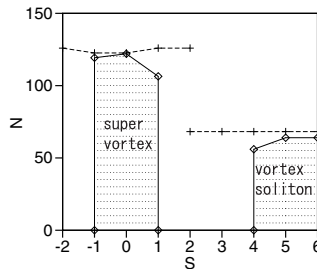


Figure 2: The right side of the diagram shows stability limits for the vortex solitons with higher vortices of the type shown in Fig. 1(c), for  $\varepsilon = 3$ . Above the critical norm (crosses), each soliton in the patterns collapses. The rings are stable in the shaded areas below the borders shown by rhombuses. In particular, the vortex with  $S = 4$  is definitely stable, while the one with  $S = 3$  is marginally unstable. The left side shows the same limits for densely-packed supervortices of the type displayed in Fig. 3, with  $\varepsilon = 10$ . The supervortices are stable in the shaded area, which actually includes only  $S = \pm 1$  and  $S = 0$ .

Next, we investigate supervortices. To this end, we built a closed array of 12 compact vortices with  $s = 1$  surrounding an empty cluster of four cells, imprinting the global vorticity onto it the same way as above (unlike the free space, where the vortex solitons is always unstable against azimuthal perturbations, in the lattice it may be completely stable, if taken below the collapse threshold [3, 4]). The resulting stationary patterns are, to the best of our knowledge, the first example of “supervortex” structures on lattices. On the contrary to the vortex rings considered above, the supervortices corresponding to  $S$  and  $-S$  are *not* equivalent. In the same case, the supervortices with  $S = -1$  and  $|S| = 2$  are stable too, the ones with  $|S| > 3$  are unstable, and the supervortices with

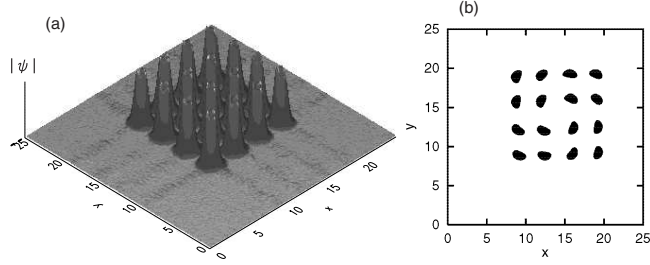


Figure 3: A densely-packed stable supervortex with  $\varepsilon = 10$ ,  $S = -1$  and  $N = 74.01$ . (a) The plot of  $|\psi(x, y)|$ . (b) The area with  $\text{Re}\{\psi(x, y)\} > 0.2$  is shaded, to highlight the vortex structure of the pattern, corresponding to  $S = -1$ .

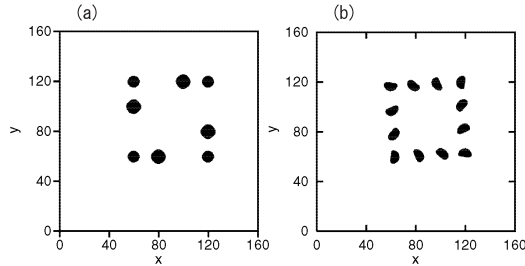


Figure 4: Stable vortex patterns in the photorefractive model (2), with  $I_0 = 0.5$  and  $K = \pi/10$ . (a) A vortex soliton with  $N = 438.7$  and  $S = 4$ . (b) A supervortex with  $N = 938.7$  and  $S = -1$ . The area with  $\text{Re}\{\psi(x, y)\} > 0.1$  is shaded, to highlight the vortex structures.

$|S| = 3$  are marginal. We have also constructed the simplest supervortices, composed of four small vortices which cover four adjacent cells of the square lattice (not shown here). It was found that such arrays are stable with  $S = 0$ , unstable with  $|S| = 2$  (actually, these are *vortex quadrupoles*), and marginal with  $S = \pm 1$ .

The stability of the supervortices composed of 12 or 4 individual vortex solitons suggest that all the supervortices with the phase difference  $\Delta\phi$  between adjacent individual vortices are *unstable* in the case of  $\Delta\phi > \pi/2$ , and they may be stable if  $\Delta\phi < \pi/2$ , exactly opposite to the vortex rings considered above. This property can be understood too: the sign of the interaction between compact vortex solitons differs from that for their zero-spin counterparts by the factor of  $(-1)^s$  [21]. Therefore, contrary to the solitons with  $s = 0$  in the ring patterns considered above, the adjacent vortices with  $s = 1$  in the supervortex patterns *repel* each other, provided that  $\Delta\phi < \pi/2$ , which gives them a chance to form stable bound states on the lattice, as per Ref. [20].

Supervortices may also exist in a densely-packed form, without the inner

hole. As shown in Fig. 3(a), it is possible to build such structures, starting with a dense set of 16 compact vortex solitons. The phase pattern corresponding to the global vorticity  $S$  was imprinted, in this case, by setting  $\Delta\phi = \pi S/2$  in the inner layer (formed of four cells), and  $\Delta\phi = \pi S/6$  in the outer one, that includes 12 cells. Results of the stability investigation for the densely packed supervortices are included in Fig. 2. In particular, the collapse threshold (above which each individual vortex collapses independently) is nearly constant,  $N_{\text{cr}}^{(\text{super})} \approx 125$ . This value can be explained similar to how it was done above for the patterns composed of the  $s = 0$  solitons, taking into regard the known critical norm for the collapse of an individual vortex soliton with  $s = 1$  [22]. The densely packed supervortices with  $|S| \geq 2$  are unstable.

The PRC model (2) gives rise to vortex solitons and supervortices very similar to those found in the GPE (1), obeying similar phase-stability conditions (of course, there is no collapse in the PRC model with the saturable nonlinearity). Figures 4(a) and (b) display a higher-order vortex soliton with  $S = 4$ , and a supervortex with  $S = -1$ . They are based on 12 single-cell  $s = 0$  or  $s = 1$  solitons which surround four empty central cells.

To summarize, we have investigated new types of vortex complexes in a class of models that includes attractive BEC in square optical lattices (OLs) and photorefractive crystals (PRCs) with the photonic lattice. The same patterns are expected in nonlinear photonic crystals and photonic-crystal fibers. The complexes include densely packed and ring-shaped higher-order vortices and supervortices. They are stable provided that the OL is strong enough. Stability limits for the total norm and vorticity of the patterns have been found and explained. The experimental creation of these vortex complexes in PRCs is quite feasible.

A larger variety of the complex vortex patterns is expected on triangular and hexagonal lattices, and, especially, in the 3D BEC model with the corresponding OL, cf. the findings made in the discrete 3D model [12]. A vast “zoo” of 3D vortex patterns was very recently reported in Ref. [23], but they were formed of dark-soliton vortex filaments in the repulsive GPE.

We appreciate discussions with B. B. Baizakov, M. Salerno, and M. Segev. The work of B.A.M. was supported, in a part, by the Israel Science Foundation through the grant No. 8006/03.

## References

- [1] J. W. Fleischer *et al.*, Nature **422**, 147 (2003).
- [2] D N. Neshev *et al.*, J. W. Fleischer *et al.*, Phys. Rev. Lett. **92**, 123904 (2004).
- [3] B. B. Baizakov, B. A. Malomed, and M. Salerno, Europhys. Lett. **63**, 642 (2003); Phys. Rev. A **70**, 053613 (2004).

- [4] J. Yang and Z. H. Musslimani , Opt. Lett. **28**, 2094 (2003); J. Opt. Soc. Am. B **21**, 973 (2004).
- [5] K. Bongs *et al.*, Phys. Rev. Lett. **83**, 3577 (1999).
- [6] B. Tanata *et al.*, Phys. Lett. A **302**, 131 (2002).
- [7] K. E. Strecker *et al.*, Nature **417**, 150(2002); L. Khaykovich *et al.*, Science **296**, 1290(2002).
- [8] J. Yang, New J. Phys. **6**, 47 (2004).
- [9] E. A. Ostrovskaya and Y. S. Kivshar, Opt. Express **12**, 19 (2004); Phys. Rev. Lett. **93**, 160405 (2004).
- [10] H. Sakaguchi and B. A. Malomed, J. Phys. B **37**, 2225 (2004).
- [11] T. J. Alexander, A. A. Sukhorukov, and Y. S. Kivshar, Phys. Rev. Lett. **93**, 063901 (2004).
- [12] P. G. Kevrekidis *et al.*, Phys. Rev. Lett. **93**, 080403 (2004); Phys. Rev. E **70**, 056612 (2004); R. Carretero-González *et al.*, Phys. Rev. Lett. **94**, 203901 (2005).
- [13] M. Soljačić, S. Sears, and M. Segev, Phys. Rev. Lett. **81**, 4851 (1998); M. Soljačić and M. Segev, Phys. Rev. E **62**, 2810 (2000); Phys. Rev. Lett. **86**, 420 (2001); A. S. Desyatnikov and Y. S. Kivshar, Phys. Rev. Lett. **87**, 033901 (2001); Y. V. Kartashov *et al.*, Phys. Rev. Lett. **89**, 273902 (2002); L. -C. Crasovan *et al.*, Phys. Rev. E **67**, 046610 (2003); D. Mihalache *et al.*, Phys. Rev. E **68**, 046612 (2003).
- [14] Y. V. Kartashov *et al.*, Opt. Lett. **29**, 1918 (2004); Phys. Rev. E **70**, 065602(R); J. Yang *et al.*, Phys. Rev. Lett. **94**, 113902 (2005).
- [15] This term is chosen due to similarity to experimentally observed “superfluxons”, i.e., dislocations in chains of fluxons trapped in annular Josephson junctions equipped with a periodic lattice of defects, B.A. Malomed and A. V. Ustinov, J. Appl. Phys. **67**, 3791 (1990).
- [16] L.-C. Crasovan *et al.*, Phys. Rev. E **66**, 036612 (2002); G. Theocharis *et al.*, Phys. Rev. Lett. **90**, 120403 (2003).
- [17] P. Xie, Z.-Q. Zhang and X. Zhang, Phys. Rev. E **67**, 026607 (2003); A. Ferrando *et al.*, Opt. Exp. **11**, 452(2003).
- [18] A. Ferrando *et al.*, Opt. Exp. **12**, 817(2004).
- [19] L. Bergé, Phys. Rep. **303**, 260 (1998).
- [20] P. G. Kevrekidis, B. A. Malomed, and A. R. Bishop, J. Phys. A Math. Gen. **34**, 9615 (2001).



- [21] B. A. Malomed, Phys. Rev. E **58**, 7928 (1998).
- [22] V. I. Kruglov, Yu. A. Logvin, and V. M. Volkov, J. Mod. Opt. **39**, 2277 (1992).
- [23] L.-C. Crasovan *et al.*, Phys. Rev. A **70**, 033605 (2004).